

## CHAPTER 5

### RESULTS

#### LITHIUM NICKEL VANADATE BY THE POLYMER PRECURSOR METHOD

##### 5.1 Introduction

In this chapter, the lithium nickel vanadate,  $\text{LiNiVO}_4$  prepared by the polymer precursor (PP) method will be discussed. The formation of dark blue colour solution along with the gas evolution was observed, and eventually turned into gelled solution until a fine powder is produced. The synthesis of this work includes the addition of polymer source, in which will produce nanosized powder for the compound.

The analysis for the thermal studies was carried out by the TGA/ DTGA studies for the obtained precursor. The XRD test was performed to determine the nature of the crystallographic structure of the compound upon different firing temperatures. The morphological observations were examined by both SEM and TEM techniques. The electrochemical reversibility of the fabricated cell was characterized by the cyclic voltammetry experiment.

## 5.2 Structural studies

### 5.2.1 X- ray diffraction (XRD)

X- ray diffraction analysis was carried out to determine the phases and the crystal structure of the sintered product. Figure 5.1 show XRD pattern for the  $\text{LiNiVO}_4$ - PP system. A weak peak located at  $2\theta = 18.6^\circ$  at [111] ratio of intensity and strong [220] peak at  $30.6^\circ$  confirms the identification of the inverse spinel  $\text{LiNiVO}_4$  product obtained from the XRD pattern [Fey and Perng, 1997; Chitra *et. al*, 2000; Kalyani *et. al*, 2002; Subramania *et. al*, 2006].

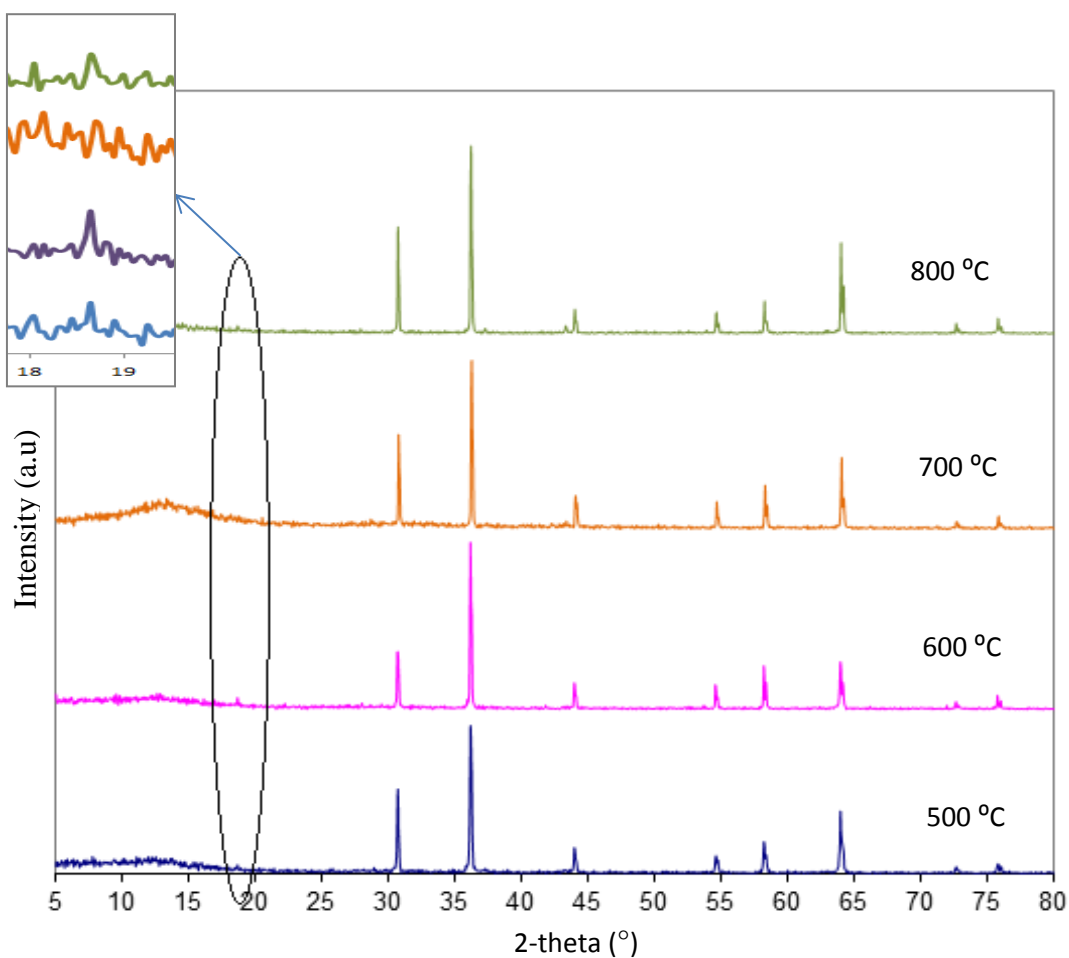


Figure 5.1: XRD pattern for the ( $\text{LiNiVO}_4$ - PP) system

The position of [220] peak is located at  $30.6^\circ$ . The XRD pattern show the presence of weak [111] Bragg line and a strong [220] line which portrays the inverse spinel  $\text{LiNiVO}_4$  [Fey and Perng, 1997]. The obtained powders at all sintering treatment found no traces of contaminants such as NiO or  $\text{Li}_3\text{VO}_6$  that usually reported in  $\text{LiNiVO}_4$  prepared by conventional solid state method [Fey *et. al*, 1997]. It is also observed that with increasing temperature, the peak intensity also increases and the peaks become sharper indicating larger particle size at elevated temperature. The resulting products for  $\text{LiNiVO}_4$  for all temperatures ( $500^\circ\text{C}$ - $800^\circ\text{C}$ ) were observed to have single phase of the compound. The continuous of crystal growth of [h k l] lines especially at [311] ratio of intensity are obtained with respect to annealing temperatures. The calculated value for the lattice constant of cubic structure for  $\text{LiNiVO}_4$ - PP system is  $8.220 \text{ \AA}$ . All peaks and the lattice constant obtained are closely matched with the JCPDS data [Card No. 38-1395]. The crystallinity nature of inverse spinel  $\text{LiNiVO}_4$  by polymer precursor method was observed at at  $500^\circ\text{C}$ ,  $600^\circ\text{C}$ ,  $700^\circ\text{C}$ ,  $800^\circ\text{C}$ , where the calculated intensity ratio of  $I_{[220]}/I_{[311]}$  is 0.57, 0.34, 0.56 and 0.57, respectively .

### 5.2.2 Crystallite size

The XRD pattern obtained were compared with the miller indices fitting based on the database. The crystallite size of the powder was calculated for each samples obtained from XRD data by using the Scherrer equation. It was found that the crystallite size between 33 nm- 48 nm was increased as the sintering temperature is increased. This behavior is rather typical for almost all crystalline materials. The material surface has more kinetic energy thus leading easier to reaching their position in the crystalline lattice at higher temperature [Kuzminykh, 2006]. This result corresponds to the

increasing peak intensities for [311] sharp lines that led to increase of crystallite size at higher sintering temperature for the system [Chaliha *et. al*, 2008]. The values of the calculated crystallite size are tabulated in Table 5.1.

**Table 5.1: Crystallite size values for the ( $\text{LiNiVO}_4$ - PP) system**

Temperature ( $^{\circ}\text{C}$ )	Crystallite Size (nm)
500	33.38
600	37.83
700	41.00
800	48.43

### 5.3 Chemical Reaction

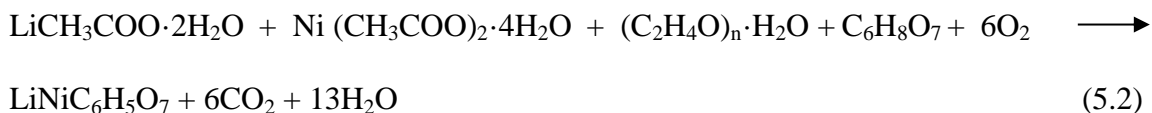
The suggested reaction of the  $\text{LiNiVO}_4$ - PP system will be discussed below. The possible reaction steps involved in the preparation of  $\text{LiNiVO}_4$  prepared by polymer precursor method are as follows:

The reaction of the citric acid,  $\text{C}_6\text{H}_8\text{O}_7$  with the  $\text{NH}_4\text{VO}_3$  will promote the formation of  $\text{V}_2\text{O}_5$  when the acid was added into the mixture:



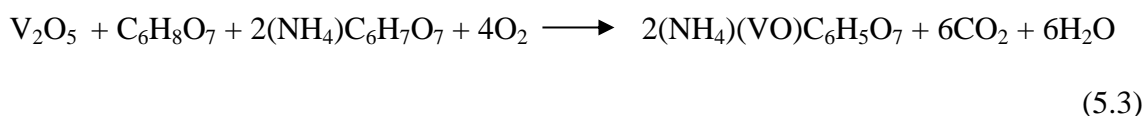
After a while, the vigorous gas evolution was observed as the result from the reaction of lithium acetate and nickel acetate with the citric acid. Subsequently, the production of

the  $\text{CO}_2$  gas and the metal complexation with the citric acid will be obtained from the reaction. Thus, after continuous heating process, the byproduct would be as follows:

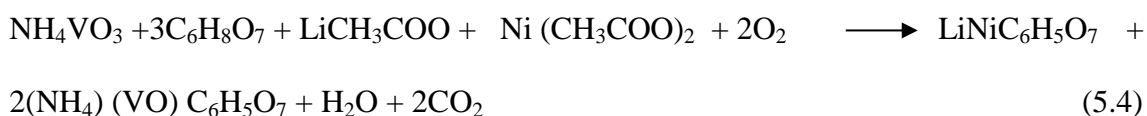


$\text{V}_2\text{O}_5$  may be oxidized by  $\text{C}_6\text{H}_8\text{O}_7$  because it is an oxidant in acidic solution. The V(V) in  $\text{V}_2\text{O}_5$  can be reduced to V(IV) with the gas evolution and forms  $(\text{VO})^{2+}$  ion.

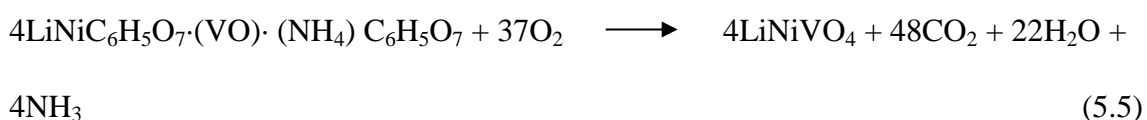
$(\text{NH}_4)(\text{VO})\text{C}_6\text{H}_5\text{O}_7$  will be produced when the  $(\text{VO})^{2+}$  ion was then reacted with  $(\text{NH}_4)\text{C}_6\text{H}_7\text{O}_7$  :



By taking all the above equations, the total reaction equation would be as follows:



Based on the equation above, the total reaction of the dried gel might be composed of  $\text{LiNiVO}_4 \cdot (\text{VO})(\text{NH}_4)\text{C}_6\text{H}_5\text{O}_7$ , as shown below. The proposed total decomposition equation in air atmosphere from the product of the total equation (5.4) can be written below:



#### 5.4 Thermogravimetric Analysis (TGA)

The dried gel has been further heated until a loose powder forming evenly throughout the prepared sample. After the precursor was gradually cooled to room temperature, the sample was sent to TGA analysis to study the thermal behaviour of the system. Figure 5.2 displays the TGA and DTGA curve for the compound prepared by polymer precursor method. The observed weight loss at room temperature until 100 °C corresponding to the evaporation of residual water left during synthesizing the precursor and decomposing of lithium acetate.

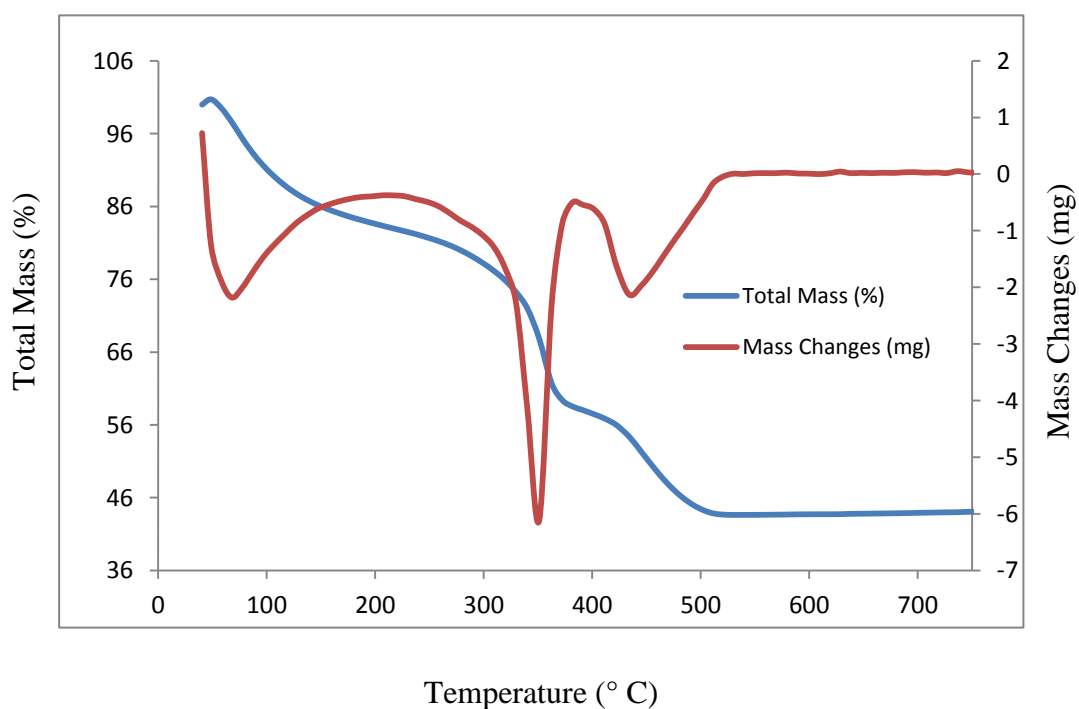


Figure 5.2: TGA and DTGA curve of the  $\text{LiNiVO}_4$ -PP precursor

The decomposition of citric acid and ammonium metavanadate happened in the temperature range from 100 °C to 200 °C, according to the melting point of both reactants. The endothermic peaks occurred in temperature range from 350 °C to 455 °C.

This reaction may be associated with the 9.83 % weight loss based on the TGA curve which may correspond to the complex decomposition of lithium, nickel and vanadium citrates. The reaction upon continuous thermal treatment at higher temperature show the decomposition process stops at temperature  $\sim 500$  °C. The residual that form after the decomposition will continue to react to form stable vanadate. The  $\text{CO}_2$  and  $\text{NH}_3$  gas will slowly reduce along the reaction. Therefore, the reaction will also promote weight loss. TGA spectrum is used to explain the chemical mechanism of  $\text{LiNiVO}_4$  phase formation during the synthesis. The total weight loss of the decomposition process is 57.3 % in this system.

## 5.5 Morphology studies

### 5.5.1 Scanning Electron Microscopy (SEM)

The scanning electron micrograph of  $\text{LiNiVO}_4$  by adding polymer source (PEG) is represented in Figure 5.3. The effect of surface morphology upon polymer intermediate does improve the physical properties to achieve better nano-crystalline powder.

Therefore, the modified method using PEG has demonstrated changes to the microstructural surface morphology as expected. Figure 5.3 (a) shows the SEM micrograph for the sample  $\text{LiNiVO}_4$ - PP at lowest temperature at exhibit flakey-looking structure with large voids. Crystal growth in Figure 5.3 (b) was observed for higher temperature at 600 °C. The cluster edges become visible at greater sintering temperature along with formation of microstructure growth as shown in Figure 5.3 (c) as it is clearly separated forming almost spherical crystalline aggregation. The particle cluster

development with visible agglomeration was present upon highest calcination temperature as shown in Figure 5.3 (d).

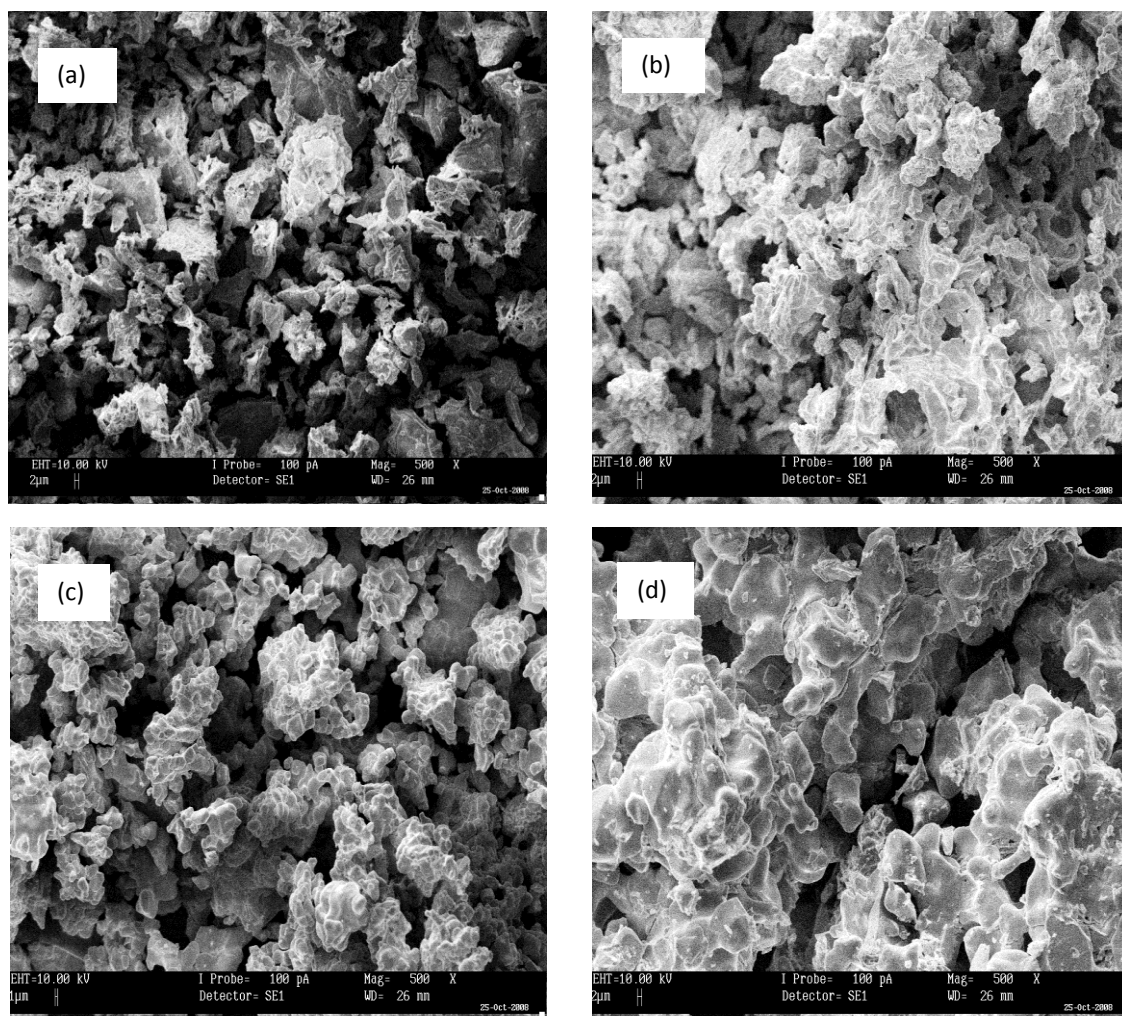
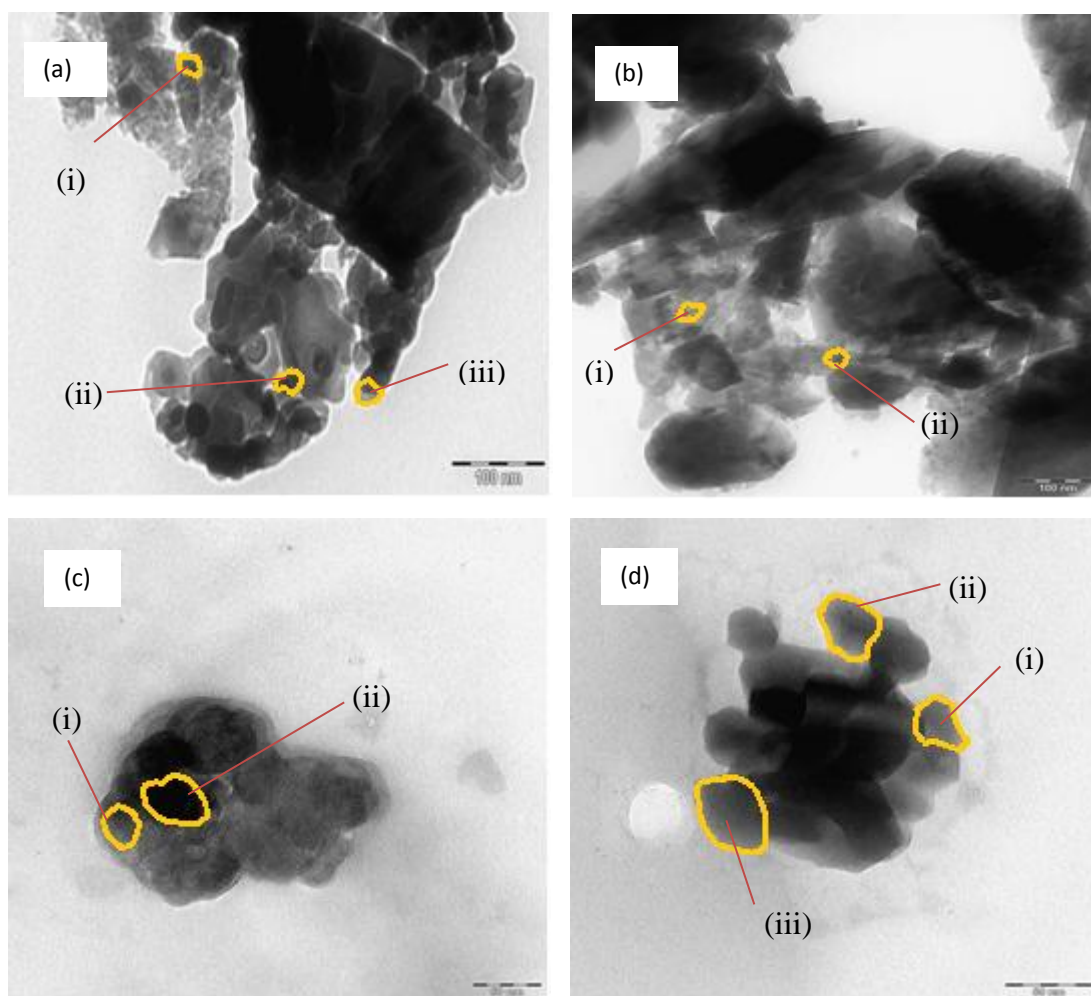


Figure 5.3: Surface morphology of  $\text{LiNiVO}_4$ - PP system (a) at 500 °C; (b) at 600 °C; (c) at 700 °C; (d) at 800 °C with 500X magnification

### 5.5.2 Transmission Electron Microscope (TEM)

The TEM morphology of the inverse spinel  $\text{LiNiVO}_4$  synthesized by polymer precursor method are presented in Figure 5.4 below. The obtained image in Figure 5.4 (a) show obvious spherical shape particles for sample fired at 500 °C. The particle size in Figure 5.4 a (i), Figure 5.4 a (ii) and Figure 5.4 a (iii) are 33.3 nm, 37.5 nm and 33.3 nm

respectively. These particles are distributed with primary diameter size of 33 nm. This result is in accordance to the crystallite size calculation obtained from the XRD data using Scherrer equation.



**Figure 5.4:** TEM images of  $\text{LiNiVO}_4$ -PP system at (a) 500 °C; (b) 600 °C; (c) 700 °C; (d) 800 °C

Figure 5.4 b (i) and Figure 5.4 b (ii) are having particle size of 40.0 nm and 30.0 nm, respectively. The particle size in Figure 5.4 c (i) and Figure 5.4 c (ii) are 33.3 nm and 50.0 nm, respectively. Visible agglomeration shown in Figure 5.4 (b) and Figure 5.4 (c) was obtained which are due to the thermal process. More densified particle clusters were exhibited having bigger crystal size agglomerated as shown in Figure 5.4 d (i- iii)

of 34.8 nm, 39.1, and 50.0 nm, respectively. The size of the particles were also expands as the temperature was increased.

### 5.6 Cyclic voltammetry (CV)

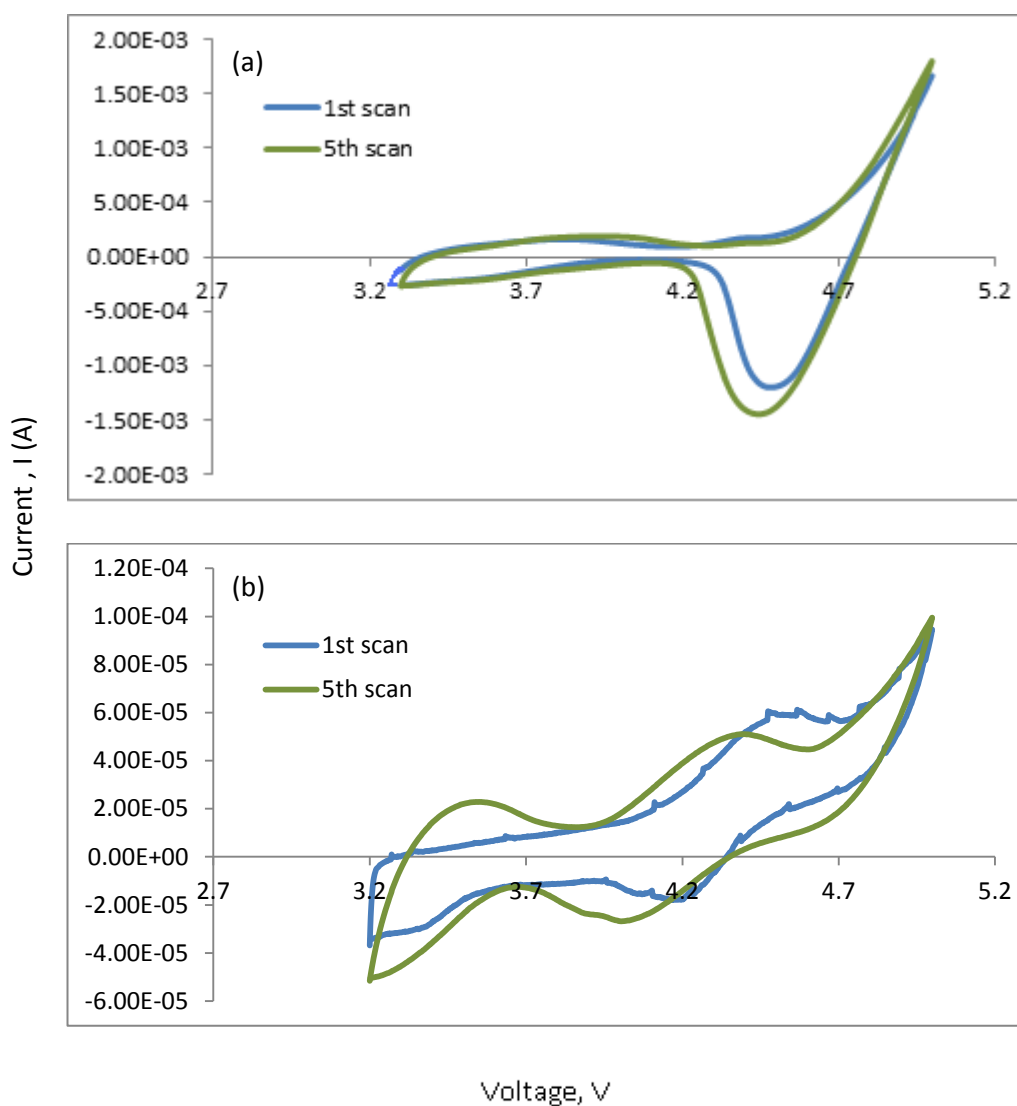


**Figure 5.5:** Cyclic voltammograms for Li/  $\text{LiNiVO}_4$ - PP electrode system in  $1 \text{ mol dm}^{-1} \text{ LiPF}_6$  in 1:2 by (vol/ vol%) EC/DMC at scan rate of  $1 \text{ mV/s}$  (a) cathode sintered at  $500 \text{ }^\circ\text{C}$ ; (b) cathode sintered at  $700 \text{ }^\circ\text{C}$

The reversibility of the Li/  $\text{LiNiVO}_4$  + PEG system is presented in Figure 5.5 above.

The cell was measured in the voltage range of 3- 5 V at the scan rate of  $1 \text{ mV/s}$ . The CV curve in Figure 5.5 (a and b) for the electrochemical system was recorded at ambient temperature for the 1<sup>st</sup> scan and 5<sup>th</sup> scan. The obtained voltammogram display the

reduction (intercalation) curve with well resolved intense peak at  $\sim 4.5$  V of lithium intercalation. Voltage shift at 4.4 V was observed at the 5<sup>th</sup> scan of the voltammogram. The voltammogram of the crystalline  $\text{LiNiVO}_4$  displays the redox nature of Li- de/intercalation process.

In this case, the reduction curve shows obvious distribution of energy for Li-intercalation. The redox voltammogram subsequently was followed by the reducing size on the 5<sup>th</sup> scan. The compound treated at higher sintering temperature ( $700^\circ\text{C}$ ) shows anodic and cathodic peak at 4.4 V and 4.2 V, respectively on the initial scan. The potential curve of the 5th cycle was reduced to 4.3 V of anodic peak. A peak at 4.0 V was also observed at cathodic scan of the cycle. The voltage difference between the charge and discharge curve shows an oxidation and reduction peaks shift to the lower potential that indicates the better reversibility after few cycling processes.

## 5.7 Summary

The polymer precursor synthesizing method for the  $\text{LiNiVO}_4$  was successfully prepared in air with the presence of the polymer source, Poly (ethylene glycol) (PEG). The thermogram curve from the TGA test show that the precursor stabilizes at around  $500^\circ\text{C}$ . The total weight loss was rather smaller (57.3 %) than the one we obtained for the pristine  $\text{LiNiVO}_4$  via sol-gel route. The additional of the polymer is to make the powder into nanosized particles. The firing temperatures were also held in the same sintering treatment ranging from  $500^\circ\text{C}$ -  $800^\circ\text{C}$ . The set of the reaction mechanism shown in this work has not been reported to the author's knowledge.

The diffractogram show no trace of contaminant as low as sintering temperature at 500 °C. The crystallite size was obtained from the FWHM, which is from the XRD data analysis and yet found to have nanosized ranged particle ranging from 33.38 nm to 48.43 nm upon rising of firing temperatures. The morphology images from the TEM analysis also confirm the formation of the nano ranged particle for the system in this work.

The presence of oxidation and reduction (redox) mechanism was also occurred in the system. These results show the intercalation and deintercalation that correspond to the insertion and extraction of the Li- ion in the cell. There was an obvious cathodic peak at ~ 4.5 V. The scan size initially having a slight increase but later it decreases at the subsequent scans. More distinct anodic and cathodic peaks were observed at compound fired at the higher temperature. In addition, the potential separations are well defined than the redox curves on the lower sintering temperature. Therefore, the reversibility was improved at higher firing temperature.